



Short communication

Synthesis of SiGe-based three-dimensional nanoporous electrodes for high performance lithium-ion batteries

Jiazheng Wang, Ning Du*, Zunqing Song, Hao Wu, Hui Zhang, Deren Yang

State Key Laboratory of Silicon Materials, Department of Materials Science and Engineering, Cyrus Tang Center for Sensor Materials and Applications, Zhejiang University, Hangzhou 310027, People's Republic of China

HIGHLIGHTS

- SiGe layer was deposited on a Cu 3D nanoporous current collector.
- The Cu–SiGe 3D electrodes show high performance as anode for Li-ion battery.
- High performance is attributed to the advantages of the electrodes' structure.

ARTICLE INFO

Article history:

Received 14 August 2012

Received in revised form

15 October 2012

Accepted 30 November 2012

Available online 10 December 2012

Keywords:

Silicon germanium

Three-dimensional

Nanoporous electrodes

Lithium-ion batteries

ABSTRACT

We demonstrate the synthesis of SiGe-based three-dimensional (3D) porous nanostructures via a template-assisted method. When tested as electrode in lithium-ion batteries, it exhibits a reversible capacity as high as 1311 mAh g⁻¹ after 45 cycles at a current density of 4 A g⁻¹. Even at a super high current rate of 16 A g⁻¹, the electrode can deliver a stable capacity of about 1047 mAh g⁻¹. The great cycling performance and superior rate capability can be attributed to the good electrical contact, fast electron transport and good strain accommodation of the 3D nanostructure of the porous electrode.

© 2013 Elsevier B.V. All rights reserved.

1. Introduction

Alloy negative electrodes for lithium-ion batteries have attracted significant industrial and scientific interest due to the high specific capacity and moderate operating voltage [1–3]. In recent papers, there is a large amount of work focusing on alloys of Si, Sb, Ge, Sn and other elements to take place of graphite as anode materials of lithium-ion batteries [4–10]. Among them, Si-based alloy materials are most appealed because Si has the highest theoretical capacity and low working potential. It is believed that alloying Si with Ge could enhance the rate capability since Ge has higher electrical conductivity (4 orders of magnitude) and lithium ion diffusivity (2 orders of magnitude) than Si [11,12]. However, two problems still remain to be overcome to meet the requirements of commercial lithium-ion batteries: (1) poor cyclability arising from

the significant volume change associated with the reversible reaction of Li; (2) low rate capability originated from long diffusion path of both electron and lithium-ion. A promising approach is to use amorphous or glass-state materials [13], as well as choosing an inactive matrix or using nano-sized alloy nanoparticles [14,15]. However, these approaches can only improve the electrochemical performance of the alloy anodes to a limited extent. It is now recognized that an efficient way to improve the electrochemical response of active materials is optimizing the electrode structure. For example, Taberna et al. have reported a Fe₃O₄-based Cu nano-architected electrode for lithium-ion batteries, which delivered long cyclic life and rate capability [16]. Nevertheless, this nano-architected electrode design is restricted by the using of AAO (Anodic Aluminum Oxide) templates, which is difficult for large-scale synthesis.

In this paper, we report the synthesis of a new type of SiGe-based 3D electrodes via a simple method. The 3D nano-architected porous electrodes have extremely high-rate capability and excellent capacity retention.

* Corresponding author. Tel.: +86 571 87953190; fax: +86 571 87952322.

E-mail address: dna1122@zju.edu.cn (N. Du).

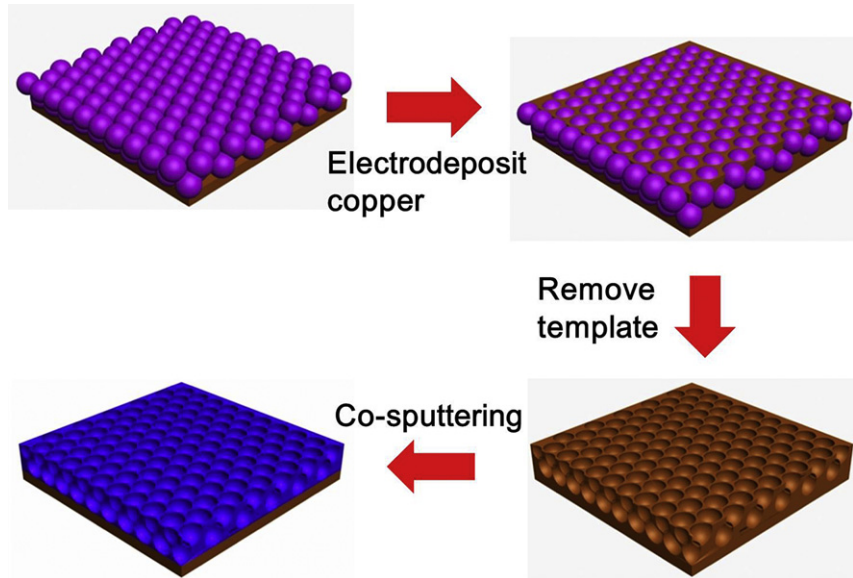


Fig. 1. (a) Schematic illustration for large-scale synthesis of the SiGe-based nanoporous 3D electrode.

2. Experiment section

2.1. Growth of silica opal-like templates

Silica nanoparticles with a diameter of 250 nm were synthesized according to a modified Stöber method [17]. The spheres were meticulously cleaned by centrifuging, decanting, and re-dispersing in ethanol. Then, the 500 μL of as-prepared silica–ethanol solution was dispersed on a mechanical polished Cu substrate. The wafer is spin-coated at 1000 rpm on a standard spin-coater for 30 s. The

thickness of this layer can be varied by the number of spin-coating steps. The fabricated colloidal crystal was annealed at 95 °C for 2 h before Cu electrodeposition.

2.2. Synthesis of nanoporous three-dimensional Cu current collector

Cu nanoporous 3D current collector was fabricated by cathodic electrodeposition through the above-mentioned templates. The electrochemical cell consisted of a working electrode (Cu Substrate

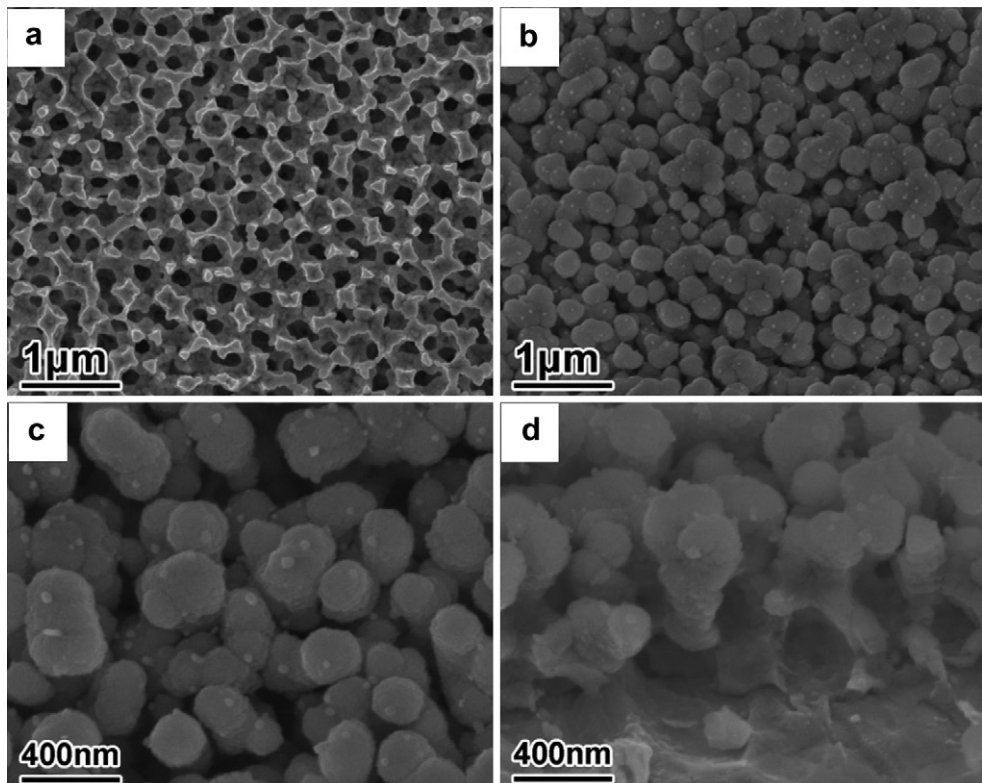


Fig. 2. (a) SEM image of the as-prepared Cu nanoporous 3D current collector; (b), (c) Top-view and (d) cross-section SEM images of the SiGe-based nanoporous 3D electrode.

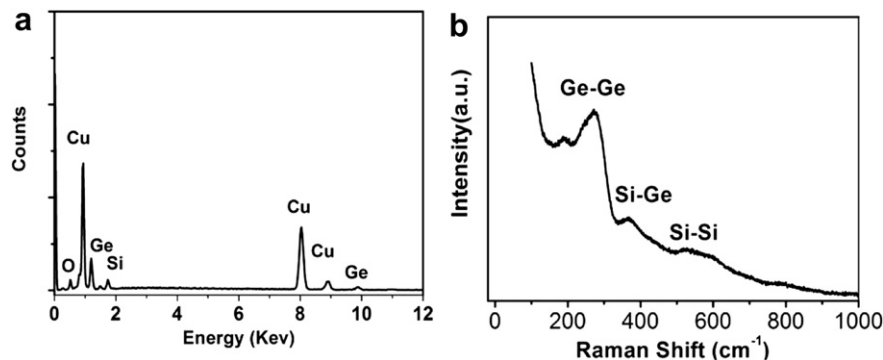


Fig. 3. (a) EDX pattern and (b) Raman analysis of the SiGe-based nanoporous 3D electrodes.

with silica template), a carbon rod counter electrode, and an Ag|AgCl reference electrode. A solution with $\text{CuSO}_4 \cdot 5\text{H}_2\text{O}$ 100 g L⁻¹, $(\text{NH}_4)_2\text{SO}_4$ 10 g L⁻¹ and diethylenetriamine (DETA) 40 g L⁻¹ was used as the electrolyte. The deposition of Cu was performed under galvanostatic conditions at a constant current of 3 mA cm⁻² for desired time. After deposition, the as-prepared samples were taken out from the electrolyte, immersed in 10% HF solution for 30 min to remove silica templates, rinsed several times with deionized water and then stored into a glove box filled with argon atmosphere.

2.3. SiGe alloy deposition

SiGe film was deposited on the surface of Cu 3D nanoporous current collector by the co-sputtering of a 99.99% pure Ge target and a 99.999% pure Si target at a working pressure of 3 Pa for 30 min. The sputtering power of the Si and Ge were 80 W and 40 W, respectively. The substrates were kept at 200 °C. The chemical compositions and element distributions of the SiGe electrodes were examined using energy-dispersive spectroscopy (EDS).

2.4. Characterization and electrochemical measurement

The Raman experiments were performed with a HR800 Raman spectrometer using the 514 nm line of an Ar ion laser operated at 10 mW. The morphology and structure of the obtained samples were examined by scanning electron microscopy (SEM HITACH S4800) with an energy-dispersive X-ray spectrometer (EDX). Electrochemical measurements were performed by coin type cells (CR2025) which were assembled in a glove box (Mbraun, labstar, Germany) under an argon atmosphere by directly using the final-products as the anodes. Lithium foil is used as both counter and reference electrodes and the electrolyte solution was 1 mol dm⁻³ solution of LiPF₆ in ethylene carbonate (EC) and Dimethyl carbonate (DMC) (1:1 by volume). Finally, the cells were then aged for 12 h before measurements. A galvanostatic cycling test of the assembled cells was carried out on a Land CT2001A system. Cyclic voltammetry (CV) were recorded on an Arbin BT 2000 system at a scan rate of 0.1 mV s⁻¹.

3. Results and discussion

An overview of the synthetic route for SiGe-based 3D nanoporous electrodes is shown in Fig. 1. Briefly, the typical synthetic procedure involves in four steps: 1) growth of silica opal-like template on a Cu substrate; 2) deposition of Cu through the template; 3) remove the template in diluted hydrofluoric acid; 4) deposit SiGe alloy via a co-sputtering method. Fig. 2a shows a representative scanning electron microscopy (SEM) image of the

nano porous 3D Cu current collector. It can be observed that the Cu current collector presents the ordered porous structure of uniformly distributed holes with diameters of about 200 nm. Fig. 2b, c shows the top view SEM images of the nanoporous Cu current collector supported by SiGe with a sputtering time of 30 min. The morphology of the 3D electrode seems to be composed of many densely packed dome-shapes at the top, for mass SiGe film was formed onto the wall of the first layer of the 3D Cu network. Fig. 2d shows its cross-section SEM image, from which we could notice that the bottom of the 3D Cu current collector has also been coated, indicates the successful fabrication of the SiGe-based 3D nanoporous electrodes. Energy dispersive X-ray spectroscopy (EDX) was carried out to verify the composition of the amorphous coating layer (Fig. 3a). The Si, Ge and Cu are detected and expected to come from SiGe alloy and the substrate, respectively. The EDX analysis also shows that the mole ratio of Si to Ge is about 3:2. The ex-situ Raman spectrum of the as-prepared nanoporous electrodes is shown in Fig. 3b, the result exhibits the peaks near 262, 362, 520 cm⁻¹, which is corresponding to the Ge–Ge, Si–Ge and Si–Si bond, respectively. The EDX and Raman results further confirm the deposition of SiGe layer.

The electrochemical performance of the SiGe alloy-based nanoporous 3D electrodes was first evaluated by cyclic voltammetry (CV). Fig. 4 shows the second curves in the potential window of 0.01–1.2 V at a scan rate of 0.1 mV s⁻¹. The cathodic sweep curve displays two peaks at around 0.16 and 0.33 V, corresponding to the formation of alloy phases, while the peaks near 0.36 and 0.5 V could be ascribed to dealloying of Li–Ge and Li–Si alloys. The results agree well with the previous reports [8]. Fig. 5a presents the discharge capacity versus cycle numbers for the as-prepared 3D electrodes between 0.01 and 1.2 V at a constant current density as high as 4 A g⁻¹. It can be seen that the discharge of the first cycle shows a high capacity of about 3100 mAh g⁻¹, the discharge

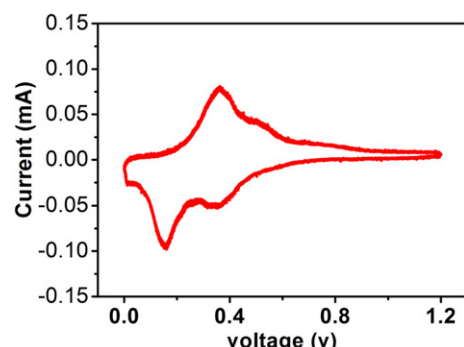


Fig. 4. The second CV curves of the SiGe-based nanoporous 3D electrode.

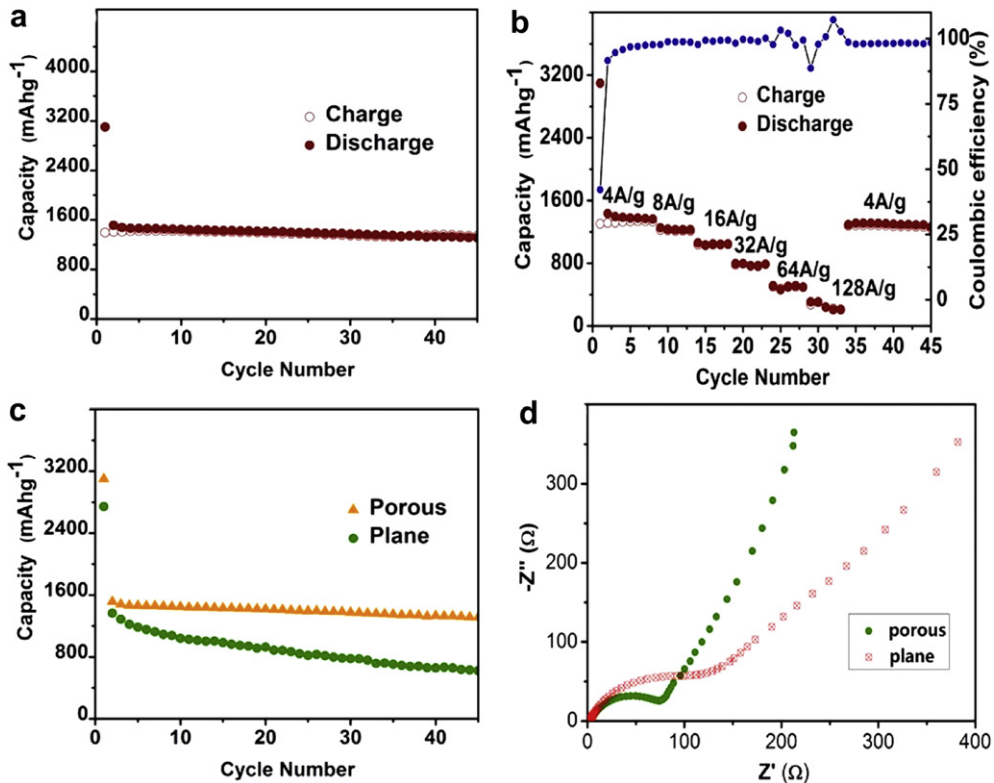


Fig. 5. (a) Discharge and charge capacities versus cycle numbers for the SiGe-based nanoporous 3D electrode at the current density of 4000 mA g^{-1} ; (b) Cycling performance at various C rates of the SiGe-based nanoporous 3D electrode; (c) Cycling performance for the three-dimensional electrode and planar electrode at the same current density; (d) Nyquist plot for the planar electrode and 3D electrode.

capacities of the electrode in the 10th, 20th and 30thcycles are $1447, 1416, 1372 \text{ mAh g}^{-1}$ respectively. A reversible capacity as high as 1311 mAh g^{-1} after 45 cycles with 86.65% capacity retention of the second discharge capacity can be observed. Recently, Taeseup Song et al. reported the synthesis of Si/Ge double-layered nanotube array electrode, which exhibit a charge capacity of about 1310 mAh g^{-1} after 50 cycles at a current of 0.2 C [12]. The capacity is comparable with our results. However, considering our current density (1.25 C versus 0.2 C) is much larger, we believe that SiGe-based 3D electrodes reported here is very attractive. Fig. 5b shows the variation of the discharge and charge capacities versus cycle numbers. As evidenced, the electrode delivers a good fraction of its capacity and operates with a stable cycling response. For instance, it exhibits the discharge capacity of $1378, 1228, 1047$, and 769 mAh g^{-1} at $4, 8, 16$ and 32 A g^{-1} , respectively. Even at a current density as high as 64 A g^{-1} , the electrode can deliver a stable capacity of about 513 mAh g^{-1} . Once upon decreasing the current rate from 128 A g^{-1} to 4 A g^{-1} , the capacity of the electrode could be restored to its original value of $\sim 1305 \text{ mAh g}^{-1}$, indicating the superior rate capability of the SiGe-based nanoporous 3D electrodes. We believe that the excellent rate performance can be attributed to its unique architecture: first, the porous structure allows for good accommodation of the volume change during cycling; second, porous structure ensures a large contact area between SiGe alloy and Cu current collector, and thus enhances the conductivity of the SiGe; Third, electrolyte-filled electrolyte pore enables an easy diffusion of the lithium ion; besides, the Cu interconnected 3D network gives a short electron diffusion path and efficient electron transport.

In order to intuitively illustrate the advantages of SiGe-based nanoporous 3D electrodes, electrochemical performance of the

SiGe film deposited directly on a plane Cu substrate was tested under the same condition for comparison. It can be seen in Fig. 5c that the capacity of the planar electrode decreases to 623 mAh g^{-1} after 45 cycles at a current density of 4 A g^{-1} , corresponding to 45.6% capacity retention of the second capacity. Obviously, the SiGe-based nanoporous 3D electrode shows the better electrochemical performance than the corresponding planar electrode. The AC impedance measurements (Fig. 5d) were performed on the above-mentioned two electrodes after 5 cycles. The charge transfer resistance is responsible for the observed chord of the arc as a consequence of the charge transfer process at the alloy/electrolyte interface. It is clear that the diameter of the semicircle in the SiGe-based 3D electrode is significantly smaller than that of the planar electrodes, revealing lower charge-transfer impedances. It is indicated that the good conductivity and accommodation of the volume change of the nanoporous 3D electrode should be responsible for the enhanced performance.

4. Conclusion

In summary, a Cu nanoporous 3D structure was synthesized via silica opal-like templates on a Cu substrate, which was subsequently deposited by SiGe layer, resulting in the SiGe-based nanoporous 3D electrodes. When used as the anode materials of Li-ion batteries, the 3D electrodes exhibited the high reversible capacity with superior rate performance, which was better than corresponding planar electrode. It is believed that the excellent electrochemical performance could be attributed to the unique nanoporous 3D structure that could efficiently buffer the volume change, facilitate the fast transport of electron and ensures a large contact area between the SiGe layer and current collector.

Acknowledgment

The authors would like to appreciate the financial support from the 863 Project (No. 2011AA050517), NSFC (No. 51002133) and Innovation Team Project of Zhejiang Province (2009R50005).

References

- [1] W. Zhang, J. Power Sources 196 (2011) 13–24.
- [2] Z. Chen, V. Chevrier, L. Christensen, J. Dahn, Electrochim. Solid-State Lett. 10 (2004) A310–A314.
- [3] W. Zhang, J. Power Sources 196 (2011) 877–885.
- [4] H. Kim, J. Choi, H. Sohn, T. Kang, J. Electrochim. Soc. 146 (1999) 4401–4405.
- [5] T. Li, Y. Cao, X. Ai, H. Yang, J. Power Sources 184 (2008) 473–476.
- [6] C. Park, H. Sohn, J. Electrochim. Soc. 157 (2010) A46–A49.
- [7] O. Mao, R. Dunlap, J. Dahn, J. Electrochim. Soc. 146 (1999) 405–413.
- [8] J. Hassoun, S. Panero, G. Mulas, B. Scrosati, J. Power Sources 171 (2007) 928–931.
- [9] S. Matsuno, M. Noji, M. Nakayama, M. Wakihara, Y. Kobayashi, H. Miyashiro, J. Electrochim. Soc. 155 (2008) A151–A157.
- [10] T. Sarakonsri, C. Johnson, S. Hackney, M. Thackeray, J. Power Sources 153 (2006) 319–327.
- [11] J. Wang, N. Du, H. Zhang, J. Yu, D. Yang, J. Power Sources 208 (2012) 434–439.
- [12] T. Song, H. Cheng, H. Choi, J. Lee, H. Han, D. Lee, D. Yoo, M. Kwon, J. Choi, S. Doo, H. Chang, J. Xiao, Y. Huang, W. Park, Y. Chung, H. Kim, J. Rogers, U. Paik, ACS Nano 6 (1) (2012) 303–309.
- [13] L. Fang, B.V.R. chowdari, J. Power Sources 97–98 (2001) 181–184.
- [14] G. Wang, L. Sun, D. Bradhurst, S. Zhong, S. Dou, H. Liu, J. Alloys Compd. 306 (2000) 249–252.
- [15] L. Shi, H. Li, Z. Wang, X. Huang, L. Chen, J. Mater. Chem. 11 (2001) 1502–1505.
- [16] L. Taberna, S. Mitra, P. Poizot, P. Simon, J.M. Tarascon, Nat. Mater. 5 (2006) 567–573.
- [17] W. Stöber, A. Fink, E. Bohn, J. Colloid Interface Sci. 26 (1968) 62–69.